

# Solid-Phase Synthesis of Co<sub>7</sub>Sm<sub>2</sub>(110) Epitaxial Nanofilms: Structural and Magnetic Properties

V. S. Zhigalov<sup>a</sup>, V. G. Myagkov<sup>a</sup>, L. A. Solov'ev<sup>b</sup>, G. N. Bondarenko<sup>b</sup>, and L. E. Bykova<sup>a</sup>

<sup>a</sup> Kirensky Institute of Physics, Siberian Branch, Russian Academy of Sciences,  
Akademgorodok, Krasnoyarsk, 660036 Russia  
e-mail: zhigalov@iph.krasn.ru

<sup>b</sup> Institute of Chemistry and Chemical Technology, Siberian Branch, Russian Academy of Sciences,  
Krasnoyarsk, 660036 Russia

Received July 24, 2008

The solid-phase synthesis of the Co<sub>7</sub>Sm<sub>2</sub> and Co<sub>17</sub>Sm<sub>2</sub> magnetically hard phases in Co/Sm/Co(110) epitaxial film systems has been experimentally investigated. The Co<sub>7</sub>Sm<sub>2</sub> phase is first formed at the Sm/Co interface at a relatively low (~300°C) temperature. As the annealing temperature increases to ~450°C, the Co<sub>17</sub>Sm<sub>2</sub>(110) phase grows epitaxially on the Co<sub>7</sub>Sm<sub>2</sub>(110) phase. The saturation magnetization and biaxial anisotropy constant in the samples vary with the formation of the Co<sub>7</sub>Sm<sub>2</sub> and Co<sub>17</sub>Sm<sub>2</sub> phases. Investigations of the solid-phase synthesis in the nanofilms reveal the existence of a new structure phase transition at 300°C in the Co–Sm system with a high cobalt content.

PACS numbers: 75.50.Vv, 75.70.Ak, 81.15.Np

DOI: 10.1134/S0021364008180100

## INTRODUCTION

Owing to the large values of the anisotropy field, saturation magnetization, and Curie temperature, Co–Sm materials have huge potential for manufacturing permanent bulk and film magnets. The high Curie temperature makes the Co–Sm system unique in high-temperature applications. Large uniaxial magnetocrystalline anisotropy, which governs the easy axis direction and is responsible for a high coercivity, makes it possible to use Co–Sm films in various microelectromechanical systems and as media for the writing and storage of information with a high density [1–4]. At present, epitaxial Co–Sm films deposited using various technological methods (ion beam, magnetic sputtering, etc.) on oriented layers are actively investigated [5–7]. Considerable efforts are focused on the investigation of exchange spring magnets consisting of multilayers, where magnetically hard Co–Sm and magnetically soft Co and Co–Nd phases are exchange coupled with each other [5, 6]. Deposition on single crystalline substrates leads to various orientation relations and, therefore, makes it possible to govern the magnetic properties of these samples. Although high-quality epitaxial magnetically hard Co<sub>5</sub>Sm, Co<sub>17</sub>Sm<sub>2</sub>, and Co<sub>7</sub>Sm<sub>2</sub> films are produced using various methods [5–7], the conditions of the formation of these phases remain poorly studied and their solid-phase synthesis has not been altogether studied. In this work, the experimental results for the solid-phase synthesis of the Co<sub>7</sub>Sm<sub>2</sub> and Co<sub>17</sub>Sm<sub>2</sub> phases in Co/Sm/Co(110) film systems, as well as the character of their epitaxial growth and their orientation

relations, are reported for the first time. The initiation temperatures are determined and possible synthesis mechanisms are discussed.

## SAMPLES AND EXPERIMENTAL PROCEDURE

Initial Co/Sm/Co(110) film structures were manufactured using the method of thermal evaporation and condensation on a MgO(001) single crystal substrate in a vacuum of 10<sup>-6</sup> Torr. The first Co layer 150 nm in thickness was deposited at a temperature of 220–250°C. At these temperature, α-Co(110) crystallites grow on the MgO(001) surface in two orientations with the *c* axis coinciding with the [100] and [010] directions. The subsequent Sm and Co layers 95 and 20 nm in thickness, respectively, are deposited at room temperature in order to avoid a reaction between the layers. At these relations between the thicknesses, the resulting samples correspond to a nominal Sm content of about 20 at %. The thin upper Co layer was deposited in order to protect against the oxidation of the Sm film. To prevent the possible oxidation of Sm, the preliminary sputtering of gettered substances (SiO and Cr) in a chamber was performed and a high rate of Sm condensation (higher than 10 nm/s) was used.

The saturation magnetization  $M_S$  and biaxial anisotropy constant  $K_2$  were measured using the torsion torque method with a maximum magnetic field of 18 kOe. To determine the thicknesses of the Sm and Co layers, the X-ray fluorescence analysis was used. X-ray

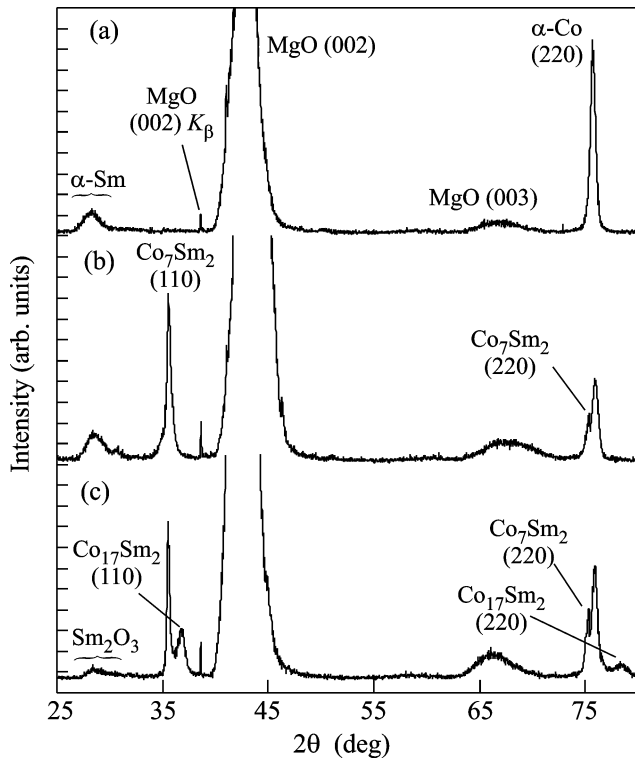


**Fig. 1.** X-ray spectra for the Co–Sm film structure (a) in the initial state and after annealing at temperatures of (b) 350 and (c) 500°C.

investigations of the epitaxial orientation of the formed phases and their identification were performed on a PANalytical X'Pert PRO diffractometer with a PIXcel detector with the use of  $\text{CuK}\alpha$  radiation monochromatized by the secondary graphite monochromator. The initial Co/Sm/Co(110)/MgO(001) samples are annealed in a temperature range from 100 to 600°C with a step of 50°C with 30-min aging at each temperature.

## EXPERIMENTAL RESULTS

Figure 1 shows the X-ray spectra for the three-layer film structure in the initial state and after annealing at temperatures of 350 and 500°C. The diffraction reflections from the initial Co/Sm/Co(110)/MgO(001) sample seen in Fig. 1a contain only the Co(220) peak, which indicates the epitaxial growth of the first  $\alpha\text{-Co}(110) \parallel \text{MgO}(001)$  layer. The type and orientation

$$\begin{aligned} \text{Co}_7\text{Sm}_2(110)[100] \parallel \alpha\text{-Co}(110)[100] \parallel \text{MgO}(001)[100], \\ \text{Co}_7\text{Sm}_2(110)[100] \parallel \alpha\text{-Co}(110)[100] \parallel \text{MgO}(001)[010]. \end{aligned} \quad (2)$$

The diffraction pattern from the film annealed at 500°C contains not only the  $\text{Co}_7\text{Sm}_2$  reflections, but also the additional reflections (110) and (220), which

of the lattice in the substrate plane for Co, as well as for the formed Co–Sm phases (see Figs. 1b and 1c) were determined using the asymmetric scanning of the characteristic reflections of the film and substrate in  $\varphi$  with the inclination of the sample by the angle  $\chi$  equal to the angle between the sample surface and the expected reflection plane; the results are shown in Fig. 2. The asymmetric scanning was performed for MgO at  $2\theta = 74.77^\circ$  and  $\chi = 25.24^\circ$ , which correspond to the (113) reflection, and for Co at  $2\theta = 92.5^\circ$  and  $\chi = 31.5^\circ$ , which correspond to the (311) reflection of the fcc lattice or the (112) reflection of the hcp lattice. The scanning results presented in Fig. 2b show that the angle  $\varphi$  between the successive reflections from the Co film is  $90^\circ$ ; therefore, the crystallites of this film have the hcp lattice with two mutually perpendicular orientations of the [001] axis in the substrate plane. The shift of the angle  $\varphi$  between the (113) MgO reflection and (112) Co reflection is  $45^\circ$ , which indicates the epitaxial codirectionality of the [001] axis of the film crystallites with the [100] and [010] axes of the substrate. This corresponds to two epitaxial relations:

$$\begin{aligned} \alpha\text{-Co}(110)[100] \parallel \text{MgO}(001)[100], \\ \alpha\text{-Co}(110)[100] \parallel \text{MgO}(001)[010]. \end{aligned} \quad (1)$$

The same epitaxial relations are valid for the Co layer in the Fe/Co bilayer films [8] and in the Co/Cr multilayers [9] epitaxially growing on MgO(001). The initial samples had the biaxial anisotropy with the constant  $K_2 = 6 \times 10^5 \text{ erg/cm}^3$  indicative of the epitaxial growth of  $\alpha\text{-Co}(110)$  on MgO(001).

According to the X-ray diffraction pattern for the film structure annealed at  $T_{\text{an}} = 350^\circ\text{C}$  (see Fig. 1b), two new reflections,  $\text{Co}_7\text{Sm}_2(110)$  and  $\text{Co}_7\text{Sm}_2(220)$ , [10] are formed on the  $\alpha\text{-Co}(220)$  base during the annealing. The measurements of the biaxial magnetic anisotropy constant provide the value  $K_2 \sim 10^7 \text{ erg/cm}^3$  (see Fig. 3b). This confirms the epitaxial growth of the  $\text{Co}_7\text{Sm}_2$  phase on the  $\alpha\text{-Co}$  sample. Hence, the  $\text{Co}_7\text{Sm}_2(110)$  crystallites, as well as the  $\alpha\text{-Co}(110)$  crystallites, grow with the  $c$  axes coinciding with the [100] and [010] directions of MgO(001). The  $\theta$ – $2\theta$  scanning with the continuous rotation in the angle  $\varphi$  indicates that the remaining part of Co holds the same orientations (see Fig. 2c). These imply that the  $\text{Co}_7\text{Sm}_2(110)$  crystallites grow on the basis of the  $\alpha\text{-Co}(110)$  crystallites with the conservation of the two orientation relations

belong to the new  $\text{Co}_{17}\text{Sm}_2$  phase [11]. The presence of only two peaks, (110) and (220), of this phase also indicates its epitaxial growth. It can be assumed that the

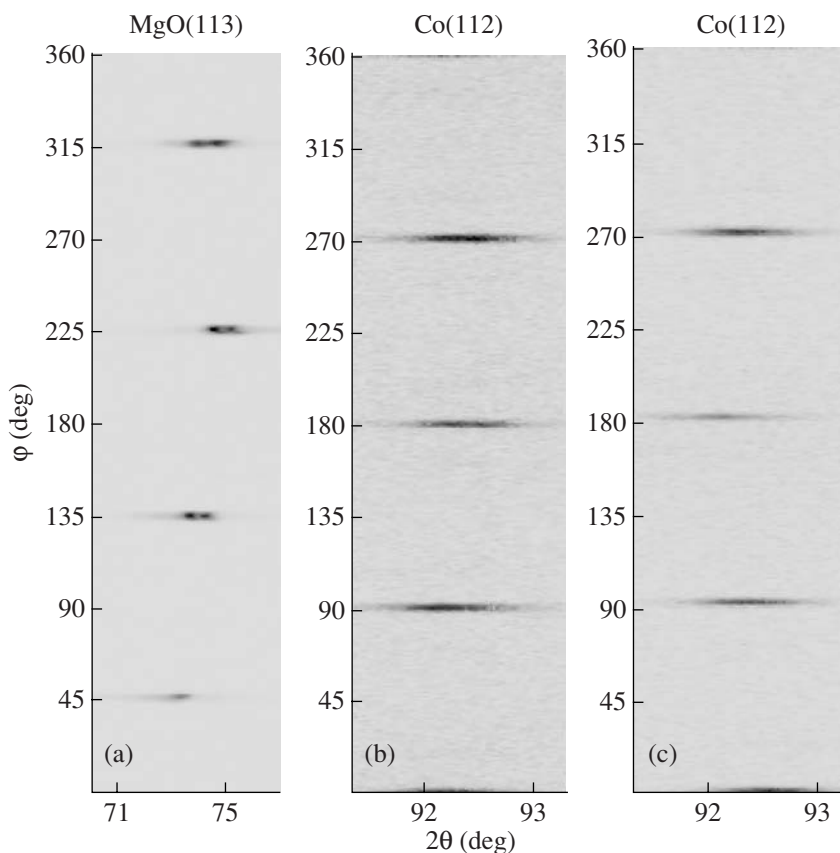


**Fig. 2.** Results of the asymmetric  $\phi$  scanning of (a) the (113) reflection from the MgO substrate and the (112) reflection from (b) the  $\alpha$ -Co films and (c) residual cobalt after annealing at a temperature of 350°C. The dark spots correspond to the diffraction relations detected at the corresponding angle  $\phi$  of the rotation about the axis perpendicular to the substrate.

$\text{Co}_{17}\text{Sm}_2(110)$  crystallites are formed on the basis of the  $\text{Co}_7\text{Sm}_2(110)$  crystallites and satisfy the orientation relations

$$\begin{aligned} \text{Co}_{17}\text{Sm}_2(110)[100] &\parallel \text{Co}_7\text{Sm}_2(110)[100] \parallel, \\ \alpha\text{-Co}(110)[100] &\parallel \text{MgO}(001)[100], \\ \text{Co}_{17}\text{Sm}_2(110)[100] &\parallel \text{Co}_7\text{Sm}_2(110)[100] \parallel, \\ \alpha\text{-Co}(110)[100] &\parallel \text{MgO}(001)[010]. \end{aligned} \quad (3)$$

The same orientation relations are characteristic of the  $\text{Co}_5\text{Sm}$ ,  $\text{Co}_{17}\text{Sm}_2$ , and  $\text{Co}_7\text{Sm}_2$  crystallites in the multilayers obtained in [5–7] in an ultrahigh vacuum under various technological conditions.

During the annealing, interlayer reaction processes in the Co/Sm/Co film structure, which are accompanied by phase and structure transformations, also gave rise to changes in the magnetic properties. Figure 3 shows the saturation magnetization  $M_S$  and biaxial anisotropy constant  $K_2$  as functions of the annealing temperature  $T_{\text{an}}$  of the Co/Sm/Co(110)/MgO(001) samples. As seen in this figure,  $M_S$  and  $K_2$  remain unchanged up to a temperature of 250°C; this behavior implies the absence of the mixing and the formation of compounds at the

Sm/Co interface. At a temperature of 300°C,  $M_S$  begins to decrease sharply and reaches a minimum at 400°C (see Fig. 3a). In contrast to the saturation magnetization,  $K_2$  increases abruptly by almost two orders of magnitude in this interval (see Fig. 3b) without a change in the easy axes. This indicates the formation of the new highly anisotropic  $\text{Co}_7\text{Sm}_2$  phase at a temperature of 300°C; this conclusion is confirmed by X-ray investigations (see Fig. 1b).

A further increase in the annealing temperature leads to the increase in the saturation magnetization  $M_S$  (see Fig. 3a) and to an insignificant increase in the constant  $K_2$  (see Fig. 3b); in this case, a new epitaxial  $\text{Co}_{17}\text{Sm}_2$  phase is formed in addition to the  $\text{Co}_7\text{Sm}_2$  phase according to X-ray measurements (see Fig. 1c).

## DISCUSSION OF THE RESULTS

Numerous investigations of the solid-phase synthesis in nanofilms and multilayers show that only one (first) phase appears at the interface at a certain temperature (initiation temperature  $T_0^1$ ), although several phases can exist according to the state diagram. At the

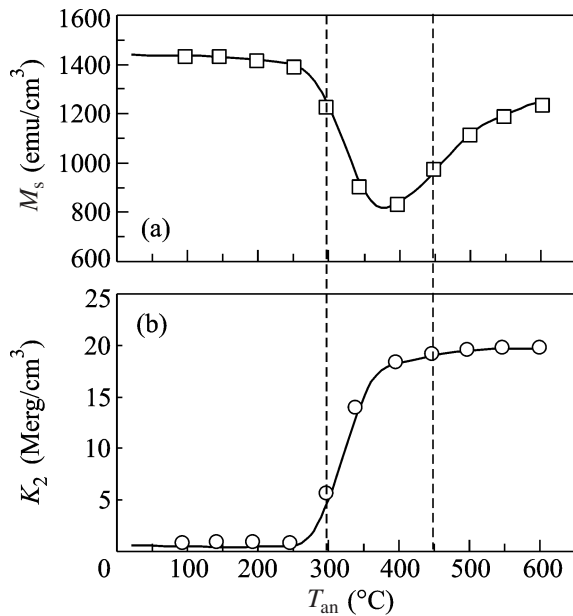


**Fig. 3.** Annealing temperature dependences of the (a) saturation magnetization and (b) effective anisotropy constant.

temperatures  $T_0^1 < T_0^2 < T_0^3$ , etc., other phases can appear, forming a phase sequence (see [12] and references therein). As shown in [13–20], at the interface of the film reagents,

(i) the first phase appears at the minimum temperature  $T_K$  of any solid-phase structural transformation in a given binary system, and

(ii) the initiation temperature  $T_0^1$  of the first phase coincides with the temperature  $T_K$  ( $T_0^1 = T_K$ ).

In particular, the solid-phase synthesis of FeS in S/Fe bilayer films is initiated at the temperature of the metal–insulator transition in FeS [13]. It was shown experimentally that the solid-phase reactions in Cu/Au films start at the Kurnakov temperature in the CuAu alloy [14]. The solid-phase synthesis of Cu<sub>2</sub>Se in Se/Cu nanofilms starts at the temperature of the superion transition in Cu<sub>2</sub>Se [15]. It was particularly surprising that the solid-phase reactions in the Ti/Ni [16, 17], Au/Cd [17, 18], Al/Ni [17, 19], and Ni/Fe [20] films start at the temperatures of the inverse martensitic transformation of the alloys in the TiNi, AuCd, AlNi, and NiFe<sub>3</sub> phases, respectively.

The above results clearly indicate that the Co<sub>7</sub>Sm<sub>2</sub> phase is first formed at the Sm/Co interface during the annealing of Sm/Co films at the nominal concentration  $C_{Co} = 80$  at %. The investigation of the solid-phase synthesis in nanofilms shows the existence of a solid-phase transformation with the temperature  $T_K^1 \sim 300^\circ\text{C}$  in the cobalt-enriched part of the binary Sm–Co system.

Analysis of orientation relations (1)–(3) for the initial  $\alpha$ -Co(110), synthesized Co<sub>7</sub>Sm<sub>2</sub>(110), and Co<sub>17</sub>Sm<sub>2</sub>(110) crystallites, respectively, implies that the Co<sub>7</sub>Sm<sub>2</sub>(110) and Co<sub>17</sub>Sm<sub>2</sub>(110) phases are formed on the basis of the  $\alpha$ -Co(110) phase. This allows the following scenario for developing the synthesis in the Sm/Co film structures. The Sm atoms at the initiation temperature  $T_0^1$  ( $\sim 300^\circ\text{C}$ ) migrate intensely to the  $\alpha$ -Co lattice and form the hexagonal Co<sub>7</sub>Sm<sub>2</sub> lattice on this basis. As a result, the Co<sub>7</sub>Sm<sub>2</sub>(110) crystallites inherit the same orientation relations with the MgO(001) substrate as the  $\alpha$ -Co(110) crystallites. However, the formation of the Co<sub>17</sub>Sm<sub>2</sub> phase at a temperature of about  $450^\circ\text{C}$  is not a result of the further processing of the solid-phase reaction in the Co/Sm/Co(110) film system; i.e., the Co<sub>17</sub>Sm<sub>2</sub> phase is not the second phase in the phase sequence. In our opinion, the Co<sub>17</sub>Sm<sub>2</sub> phase appears because a part of the Sm atoms oxidize; this is indicated by the appearance of a series of peaks in the range  $2\theta = 25^\circ$ – $35^\circ$  (see Fig. 1c). It can be assumed that, at temperatures above  $450^\circ\text{C}$ , oxygen from the substrate or remaining oxygen from the vacuum atmosphere migrates to the sample and forms samarium oxides in it.

It is known that the magnetocrystalline anisotropy, i.e., easy axes can be controlled by changing the crystallographic texture, which is determined by the texture of the initial epitaxial layer [ $\alpha$ -Co(110) in this case]. For this reason, magnetically hard Co–Sm films with the desired magnetic properties can be obtained using the solid-phase synthesis by depositing the initial Co layer on various single-crystal substrates or on single-crystal sublayers. This is very important for applications.

## CONCLUSIONS

To conclude, it has been shown that the interlayer reactions in the Co/Sm/Co(110) system promote the formation of the Co<sub>7</sub>Sm<sub>2</sub> and Co<sub>17</sub>Sm<sub>2</sub> epitaxial phases at  $T_{an} \sim 300$  and  $450^\circ\text{C}$ , respectively. The latter phase is formed due to the partial oxidation of Sm. The synthesis of the Co<sub>7</sub>Sm<sub>2</sub> phase is assumingly caused by the migration of Sm atoms to the  $\alpha$ -Co single-crystal lattice; for this reason, the Co<sub>7</sub>Sm<sub>2</sub>(110) crystallites inherit the orientation relations of the matrix. The magnetic properties of the Co/Sm/Co(110) samples change with the formation of the Co<sub>7</sub>Sm<sub>2</sub> and Co<sub>17</sub>Sm<sub>2</sub> phases. The synthesized Co–Sm phases have high biaxial anisotropy constants.

This work was supported by the Russian Foundation for Basic Research (project no. 07-03-00190) and by the program “Development of the Scientific Potentiality of the Higher Education” (project no. 2.1.1.7376).

## REFERENCES

1. L. N. Zhang, J. S. Chen, J. Ding, et al., *J. Appl. Phys.* **103**, 113908 (2008).
2. A. Walther, D. Givord, N. M. Dempsey, et al., *J. Appl. Phys.* **103**, 043911 (2008).
3. J. Zhang, Y. K. Takahashi, R. Gopalan, et al., *J. Magn. Magn. Mater.* **310**, 1 (2007).
4. D. N. Lambeth, E. M. T. Velu, and G. H. Bellesis, *J. Appl. Phys.* **79**, 4496 (1996).
5. J. Zhou, R. Skomski, Y. Liu, et al., *J. Appl. Phys.* **97**, 10K304 (2005).
6. Z. J. Guo, J. S. Jiang, J. E. Pearson, and S. D. Bader, *Appl. Phys. Lett.* **81**, 2029 (2002).
7. A. Singh, V. Neu, R. Tamm, et al., *Appl. Phys. Lett.* **87**, 072505 (2005); E. E. Fullerton, J. S. Jiang, C. Rehm, et al., *Appl. Phys. Lett.* **71**, 1579 (1997); E. E. Fullerton, J. S. Jiang, C. H. Sowers, et al., *Appl. Phys. Lett.* **72**, 380 (1998); G. Zangari, B. Lu, D. E. Laughlin, and D. N. Lambeth, *J. Appl. Phys.* **85**, 5759 (1999); A. Singh, R. Tamm, V. Neu, et al., *J. Appl. Phys.* **97**, 093902 (2005).
8. S. G. Wang, C. Wang, A. Kohn, et al., *J. Appl. Phys.* **101**, 09D103 (2007).
9. J. C. A. Huang, F. C. Tang, W. W. Fang, et al., *J. Appl. Phys.* **79**, 4790 (1996).
10. JCDPS card no. 71-0387, International Centre for Diffraction Data, 1601 Park Lane, Swarthmore, Pennsylvania, USA.
11. JCDPS card no. 65-7762, International Centre for Diffraction Data, 1601 Park Lane, Swarthmore, Pennsylvania, USA.
12. R. Pretorius, C. C. Theron, A. Vantomme, et al., *Rev. Solid. State Mater. Sci.* **24**, 1 (1999); T. Laurila and J. Molarius, *Crit. Rev. Solid. State Mater. Sci.* **28**, 185 (2003); *Thin Films-Interdiffusion and Reaction*, Ed. by J. M. Poate, K. N. Tu, and J. W. Mayer (Wiley, New York, 1978).
13. V. G. Myagkov, L. E. Bykova, V. S. Zhigalov, et al., *Dokl. Akad. Nauk* **371**, 763 (2000) [*Dokl. Phys.* **45**, 157 (2000)].
14. V. G. Myagkov, L. E. Bykova, V. S. Zhigalov, et al., *Pis'ma Zh. Éksp. Teor. Fiz.* **71**, 268 (2000) [*JETP Lett.* **71**, 183 (2000)].
15. V. G. Myagkov, L. E. Bykova, and G. N. Bondarenko, *Dokl. Akad. Nauk* **390**, 35 (2003) [*Dokl. Phys.* **48**, 206 (2003)].
16. V. G. Myagkov, L. E. Bykova, and G. N. Bondarenko, *Dokl. Akad. Nauk* **382**, 463 (2002) [*Dokl. Phys.* **47**, 95 (2002)].
17. L. E. Bykova, V. G. Myagkov, and G. N. Bondarenko, *Khim. Inter. Ushoich. Razv.* **13**, 137 (2005).
18. V. G. Myagkov, L. E. Bykova, and G. N. Bondarenko, *Dokl. Akad. Nauk* **388**, 46 (2000) [*Dokl. Phys.* **48**, 30 (2003)].
19. V. G. Myagkov, L. E. Bykova, and G. N. Bondarenko, *Dokl. Akad. Nauk* **396**, 187 (2004) [*Dokl. Phys.* **49**, 289 (2004)]; V. G. Myagkov, L. E. Bykova, S. M. Zharkov, et al., *Solid State Phenom.* **138**, 377 (2008).
20. V. G. Myagkov, V. S. Zhigalov, L. E. Bykova, et al., *J. Magn. Magn. Mater.* **305**, 334 (2006); V. G. Myagkov, V. S. Zhigalov, L. E. Bykov, et al., *J. Magn. Magn. Mater.* **310**, 126 (2007).

*Translated by R. Tyapaev*